
Revisiting Zeroth-Order Optimization for Memory-Efficient LLM Fine-Tuning: A Benchmark

Yihua Zhang^{*1} Pingzhi Li^{*2} Junyuan Hong^{*3} Jiayang Li⁴ Yimeng Zhang¹ Wenqing Zheng³
Pin-Yu Chen⁵ Jason D. Lee⁶ Wotao Yin⁷ Mingyi Hong⁴ Zhangyang Wang³ Sijia Liu¹⁵ Tianlong Chen²⁸⁹

Abstract

In the evolving landscape of natural language processing (NLP), fine-tuning pre-trained Large Language Models (LLMs) with first-order (FO) optimizers like SGD and Adam has become standard. Yet, as LLMs grow in size, the substantial memory overhead from back-propagation (BP) for FO gradient computation presents a significant challenge. Addressing this issue is crucial, especially for applications like on-device training where memory efficiency is paramount. This paper proposes a shift towards BP-free, zeroth-order (ZO) optimization as a solution for reducing memory costs during LLM fine-tuning, building on the initial concept introduced by Malladi et al. (2023). Unlike traditional ZO-SGD methods, our work expands the exploration to a wider array of ZO optimization techniques, through a comprehensive, first-of-its-kind benchmarking study across five LLM families (Roberta, OPT, LLaMA, Vicuna, Mistral), three task complexities, and five fine-tuning schemes. Our study unveils previously overlooked optimization principles, highlighting the importance of task alignment, the role of the forward gradient method, and the balance between algorithm complexity and fine-tuning performance. We further introduce novel enhancements to ZO optimization, including block-wise descent, hybrid training, and gradient sparsity. Our study offers a promising direction for achieving further memory-efficient LLM fine-tuning. Codes to reproduce all our experiments are at <https://github.com/ZO-Bench/ZO-LLM>.

1. Introduction

Fine-tuning pre-trained large language models (LLMs) has become the *de-facto* standard in the current paradigms of natural language processing (NLP) (Raffel et al., 2023; Sanh et al., 2022). First-order (FO) optimizers, *e.g.*, SGD (Amari, 1993) and Adam (Kingma & Ba, 2014), have been the predominant choices for LLM fine-tuning. However, as LLMs continue to scale, they encounter significant memory overhead due to the back-propagation (BP) required for FO gradient computation. For example, computing the gradient of the LLM OPT-13B requires $12\times$ more memory cost than the model inference. This leads to the challenge of achieving *memory-efficient fine-tuning* in LLMs. Advancements in addressing this challenge could also facilitate technological breakthroughs in related areas, such as on-device training, where memory efficiency is in high demand (Han et al., 2015; Zhu et al., 2023).

To enhance memory efficiency, an emerging solution is to replace a BP-required FO optimization method with a *BP-free* optimizer during LLM fine-tuning. This was initially proposed by Malladi et al. (2023), where the FO gradient is approximated using a finite difference of function values. Despite its new application to LLM fine-tuning, the underlying optimization principle used in Malladi et al. (2023) is commonly known as *zeroth-order (ZO) optimization*, and the function value-based gradient estimate is referred to as the ZO gradient estimate (Flaxman et al., 2005; Nesterov & Spokoiny, 2017; Duchi et al., 2015; Ghadimi & Lan, 2013; Liu et al., 2020). Malladi et al. (2023) employed the classical ZO stochastic gradient descent (ZO-SGD) algorithm (Ghadimi & Lan, 2013), termed MeZO, to fine-tune the pre-trained LLMs and leveraged the BP-free characteristics of ZO optimization to reduce memory costs. However, from the perspective of ZO optimization, in addition to ZO-SGD, many other ZO optimization methods have not yet been explored in the context of LLM fine-tuning. Thus, it remains elusive whether there are potential improvements in *accuracy* and/or *efficiency* that can be achieved through a benchmarking study of ZO optimization for LLM fine-tuning. This yields the primary question to be explored:

^{*}Equal contribution ¹Michigan State University ²The University of North Carolina at Chapel Hill ³UT Austin ⁴University of Minnesota Twin Cities ⁵IBM Research ⁶Princeton University ⁷DAMO Academy, Alibaba Group US ⁸MIT ⁹Harvard University. Correspondence to: Sijia Liu <liusiji5@msu.edu>, Tianlong Chen <tianlong@cs.unc.edu>.

(Q) *Can we establish a benchmark for ZO optimization in LLM fine-tuning, explore the overlooked optimization principles, and advance the current state of the art?*

To address (Q), our work introduces several key innovations compared to the most relevant work (Malladi et al., 2023). We explore a broader range of ZO optimization methods beyond ZO-SGD and examine various task and model types, and evaluation metrics. We conduct a detailed comparative analysis of different ZO optimization methods, shedding light on the often-overlooked forward gradient method (Ren et al., 2022) and other ZO optimization techniques in LLM fine-tuning. This benchmarking study helps reveal the pros and cons of these methods in accuracy and efficiency. Extended from the gained insights, we propose to further improve ZO optimization-based LLM fine-tuning using techniques of block-wise descent, hybrid ZO and FO training, and gradient sparsity.

In summary, our key **contributions** are listed below.

- We create the first benchmark for ZO optimization in the context of LLM fine-tuning. This benchmark includes our investigations into 6 BP-free or ZO optimization methods, 5 LLM families, 3 tasks of varying complexities, and 5 fine-tuning schemes, covering both full-parameter and parameter-efficient fine-tuning (PEFT) approaches.
- Assisted by our benchmark, we reveal a range of previously overlooked optimization principles and insights for LLM fine-tuning with ZO optimization. These include the significance of aligning tasks to enhance ZO optimization, the role of forward gradient as an LLM fine-tuning baseline, and the trade-offs between algorithm complexity, fine-tuning accuracy, query and memory efficiency.
- In addition to a holistic assessment of existing ZO optimization methods for LLM fine-tuning, we introduce novel enhancements to ZO optimization, including block-wise ZO optimization, hybrid ZO and FO fine-tuning, and sparsity-induced ZO optimization. These proposed techniques aim to improve the accuracy of ZO LLM fine-tuning while maintaining memory efficiency.

2. Related Work

Parameter-efficient fine-tuning (PEFT). Early efforts (Houlsby et al., 2019; Lin et al., 2020) involved inserting trainable adapters, which are compact feed-forward networks, between the layers of the pre-trained model. More recently, various PEFT strategies have been proposed. For instance, *Adapter*-based methods (Houlsby et al., 2019; Chen et al., 2022; Luo et al., 2023; Karimi Mahabadi et al., 2021; Pfeiffer et al., 2020) insert a few tunable yet highly compact modules into pre-trained models. *LoRA* (Hu et al., 2021a) employs trainable low-rank

weight perturbations to the pre-trained model, effectively reducing the required number of fine-tuning parameters. *Prompt-based learning* (Gao et al., 2020; Hu et al., 2021b; Tan et al., 2021) has demonstrated effectiveness in various NLP tasks. Additionally, methods like *prompt tuning* (Lester et al., 2021) and *prefix tuning* (Li & Liang, 2021) incorporate learnable continuous embeddings into the model’s hidden states to condition the frozen model for specific downstream tasks. The following work (Liu et al., 2021) demonstrates its applicability on various model scales. While these state-of-the-art PEFT techniques have significantly reduced the number of parameters required for fine-tuning, they still incur memory costs associated with caching numerous activations due to the use of back-propagation (BP) (Malladi et al., 2023).

Zeroth-order optimization. Zeroth-order (ZO) optimization is a technique that uses finite differences to estimate gradients. Such algorithms utilize function value oracle only, yet share similar algorithm structure with first-order (FO) gradient-based counterpart methods. ZO optimization usually enjoys provable (dimension-dependent) convergence guarantees, as discussed in various works (Flaxman et al., 2005; Nesterov & Spokoiny, 2017; Duchi et al., 2015; Ghadimi & Lan, 2013). These methods have drawn considerable attention due to its effectiveness in a wide range of modern machine learning (ML) challenges (Liu et al., 2020), including the adversarial attack and defense (Chen et al., 2017; Tu et al., 2019; Ye et al., 2018; Ilyas et al., 2018; Zhang et al., 2022b; Verma et al., 2023; Zhao et al., 2019; Hogan & Kailkhura, 2018; Shu et al., 2022), model-agnostic contrastive explanations (Dhurandhar et al., 2019), enhancing transfer learning through visual prompting (Tsai et al., 2020), computational graph unrolling (Vicol et al., 2023), and optimizing automated ML processes (Gu et al., 2021a; Wang et al., 2022). Beyond standard ML, it finds application in policy search in reinforcement learning (Vemula et al., 2019), network resource management (Liu et al., 2018), ML-based optimization of scientific workflows (Hoffman et al., 2022; Tsaknakis et al., 2022; Chen et al., 2024), and on-chip learning enhancements (Gu et al., 2021b).

Despite its wide range of use cases, the application of ZO optimization in ML has primarily been restricted to small model scales. This limitation is attributed to the high variance and slow convergence associated with ZO optimization, which are exacerbated by model dimensions. To scale up ZO optimization, several acceleration techniques have been proposed. These include the integration of historical data to refine ZO gradient estimators (Meier et al., 2019; Cheng et al., 2021), leveraging gradient structural information (Singhal et al., 2023) or sparsity to diminish the dependency of ZO optimization on problem size (Wang et al., 2017; Cai et al., 2022, 2021; Balasubramanian & Ghadimi, 2018; Ohta et al., 2020; Gu et al., 2021b; Chen

et al., 2024), the reuse of intermediate features (Chen et al., 2024) and random perturbation vectors (Malladi et al., 2023) in the optimization process. These advancements suggest a growing potential for the application of ZO optimization in more complex and large-scale ML problems.

BP-free training for large models. Training large models, especially LLMs, is memory-consuming due to the involved large computation graphs for BP (Ren et al., 2021; Kim et al., 2023). Thus BP-free methods have become a recent focus in the deep learning (DL) community. Forward gradient learning (Baydin et al., 2022; Ren et al., 2022; Silver et al., 2021; Belouze, 2022), built upon the forward-mode automatic differentiation (AD), provides an alternative to ZO optimization for BP-free training. Different from ZO optimization, it relies on the forward-mode AD to calculate a forward (directional) gradient. However, one main limitation of the forward gradient is its requirement of full access to the AD software and the deep model, making it less memory-efficient than ZO optimization and impractical for tackling black-box problems (Chen et al., 2024). The specifications of BP-free methods include greedy layer-wise learning (Nøkland & Eidnes, 2019), input-weight alignment (Boopathy & Fiete, 2022), forward-forward algorithm (Hinton, 2022), synthetic gradients (Jaderberg et al., 2017), BBT/BBTv2 evolutionary algorithms (Sun et al., 2022a;b), gradient guessing using special low dimensional structure of neural networks (Singhal et al., 2023) and other black-box methods which optimize the prompts (Prasad et al., 2023; Deng et al., 2022; Chai et al., 2022). Many of these algorithms are also motivated through the lens of seeking DL’s biological interpretation.

Applying ZO optimization to fine-tune pre-trained LLMs is particularly intriguing because it combines the advantages of being BP-free and utilizing pre-training. This enables the scalability of ZO optimization to large-scale LLMs while maintaining memory efficiency. MeZO (Malladi et al., 2023) introduced a scalable ZO-SGD algorithm to efficiently fine-tune LLMs with up to 60 billion parameters, achieving competitive results compared to first-order optimization methods and structured fine-tuning approaches like LoRA. They also provided theoretical insights into why ZO methods can be effective for LLMs. This opens the gateway for efficient BP-free LLM fine-tuning and largely motivates our ZO benchmark study.

3. Reviewing ZO Optimization and Beyond

This work’s core objective is to benchmark and harness the potential of ZO (zeroth-order) optimization in LLM finetuning, eliminating the need for (first-order) back-propagation (BP) during finetuning and thus achieving memory efficiency (Malladi et al., 2023). It is worth noting that the ZO optimization technique utilized in (Malladi et al., 2023) is primarily the basic version, specifically, ZO stochastic

gradient descent (ZO-SGD). There are more advanced ZO optimization methods available, as summarized in (Liu et al., 2020). Thus, this section is dedicated to reviewing a broader range of ZO optimization approaches and shedding light on the previously overlooked principles for LLM fine-tuning.

Basics of ZO optimization. ZO optimization serves as a gradient-free alternative to first-order (FO) optimization, approximating FO gradients through function value-based gradient estimates, which we call *ZO gradient estimates*, as discussed in (Flaxman et al., 2004; Nesterov & Spokoiny, 2017; Ghadimi & Lan, 2013; Duchi et al., 2015). Thus, a ZO optimization method typically mirrors the algorithmic framework of its corresponding FO optimization counterpart. However, it substitutes the FO gradient with the ZO gradient estimate as the descent direction.

Various techniques exist for performing ZO gradient estimation. In this paper, we focus on the *randomized gradient estimator (RGE)* (Nesterov & Spokoiny, 2017; Duchi et al., 2015), a method that relies on the finite difference of function values along a randomly chosen direction vector. RGE has also been used by Malladi et al. (2023) to achieve memory-efficient fine-tuning for LLMs. Its preference in LLM fine-tuning is attributed to its *query efficiency*, i.e., a low number of function queries. Given a scalar-valued function $f(\mathbf{x})$ where $\mathbf{x} \in \mathbb{R}^d$ of dimension d , the RGE (referred to as $\hat{\nabla}f(\mathbf{x})$) is expressed using central difference:

$$\hat{\nabla}f(\mathbf{x}) = \frac{1}{q} \sum_{i=1}^q \left[\frac{f(\mathbf{x} + \mu\mathbf{u}_i) - f(\mathbf{x} - \mu\mathbf{u}_i)}{2\mu} \mathbf{u}_i \right] \quad (\text{RGE})$$

where \mathbf{u}_i is a random direction vector typically drawn from the standard Gaussian distribution $\mathcal{N}(\mathbf{0}, \mathbf{I})$, q is the number of function queries, and $\mu > 0$ is a small perturbation step-size (also known as smoothing parameter). Malladi et al. (2023) employed RGE by setting $q = 1$ and $\mathbf{u}_i = \mathbf{u}$. Yet, it is worth noting that the query number q strikes a balance between the ZO gradient estimation variance and the query complexity. It has been shown in (Duchi et al., 2015; Liu et al., 2018) that the variance of RGE is roughly in the order of $O(d/q)$, where $O(\cdot)$ signifies the Big O notation.

The rationale behind RGE stems from the concept of the *directional derivative* (Duchi et al., 2015): As $\mu \rightarrow 0$ (letting $q = 1$), the finite difference of function values in (RGE) approaches $f'(\mathbf{x}, \mathbf{u}) := \mathbf{u}^T \nabla f(\mathbf{x})$, representing the directional derivative of $f(\mathbf{x})$ along the random direction $\mathbf{u} \sim \mathcal{N}(\mathbf{0}, \mathbf{I})$. Subsequently, RGE yields $\hat{\nabla}f(\mathbf{x}) \rightarrow f'(\mathbf{x}, \mathbf{u})$ as $\mu \rightarrow 0$. Moreover, the directional derivative provides us an unbiased gradient estimator of $\nabla f(\mathbf{x})$:

$$\mathbf{E}_{\mathbf{u}}[f'(\mathbf{x}, \mathbf{u})\mathbf{u}] = \mathbf{E}_{\mathbf{u}}[\mathbf{u}\mathbf{u}^T \nabla f(\mathbf{x})] = \nabla f(\mathbf{x}). \quad (1)$$

With the above background, the RGE $\hat{\nabla}f(\mathbf{x})$ can be interpreted as an approximation of the FO gradient $\nabla f(\mathbf{x})$ using the directional derivative.

Forward gradient: A missing BP-free baseline in LLM fine-tuning. As a byproduct of connecting RGE to (1), we obtain the directional derivative-based gradient estimate, $\nabla f(\mathbf{x}) \approx f'(\mathbf{x}, \mathbf{u})\mathbf{u}$, which is known as the *forward gradient* (**Forward-Grad**) (Baydin et al., 2022; Ren et al., 2022). Different from RGE that relies solely on the finite difference of function values, Forward-Grad requires the use of forward mode automatic differentiation (AD) but eliminates the need for the backward evaluation in the implementation of deep model fine-tuning or training. In other words, Forward-Grad is BP-free and can serve as another alternative gradient estimation method that improves the memory efficiency of LLM fine-tuning. We stress that Forward-Grad is a possibly overlooked BP-free optimizer. Given its unbiasedness as shown in (1), it could serve as an upper performance bound for ZO optimization in theory.

A focused spectrum of ZO optimization methods. Next, we provide a brief overview of the ZO optimization methods to be focused on in this work. Specifically, we will include: **ZO-SGD** (Ghadimi & Lan, 2013) that Malladi et al. (2023) has employed for LLM fine-tuning, ZO-SGD using sign-based gradient estimation (**ZO-SGD-Sign**) (Liu et al., 2019a), ZO-SGD with momentum (**ZO-SGD-MMT**) (Malladi et al., 2023), ZO-SGD with conservative gradient update (**ZO-SGD-Cons**), and the ZO variant of the Adam optimizer (**ZO-Adam**) (Chen et al., 2019).

The aforementioned methods can be unified into the following generic optimization framework in solving $\min_{\mathbf{x}} f(\mathbf{x})$:

$$\mathbf{x}_{t+1} = \mathbf{x}_t - \eta_t h(\hat{\nabla} f(\mathbf{x}_t)), \quad (2)$$

where \mathbf{x}_t denotes the updated solution at the t th iteration, $\eta_t > 0$ is the learning rate, and $h(\cdot)$ is a certain descent direction post-processing operation. In (2), we omit the inclusion of the stochastic mini-batch for empirical risk minimization for ease of presentation. For instance, ZO-SGD can be expressed as (2) when $h(\hat{\nabla} f(\mathbf{x})) = \hat{\nabla} f(\mathbf{x})$. Similarly, ZO-SGD-Sign can be derived if $h(\hat{\nabla} f(\mathbf{x})) = \text{sign}(\hat{\nabla} f(\mathbf{x}))$, where $\text{sign}(\cdot)$ represents element-wise sign operation. Another example is ZO-SGD-Cons by setting $h(\hat{\nabla} f(\mathbf{x})) = \arg \min_{\mathbf{g} \in \{\mathbf{0}, -\hat{\nabla} f(\mathbf{x}), \hat{\nabla} f(\mathbf{x})\}} f(\mathbf{x}_t + \eta_t \mathbf{g})$. We refer readers to Appx. B for more algorithmic details of (2) as applied to the ZO optimization approaches we covered.

Our rationale for selecting the aforementioned ZO optimization approaches for LLM fine-tuning is based on two key considerations: (1) We prioritize ZO optimization methods that require minimal modifications to the existing FO optimizer, ensuring ease of implementation for LLM fine-tuning. (2) We focus on methods with distinct algorithmic characteristics, allowing us to explore a diverse range of optimization strategies for improving LLM performance. Regarding (2), we include ZO-SGD-Sign as it employs 1-bit gradient quantization and represents one of the simplest

Table 1. Test accuracy (%) of pretrained Roberta-Large model fine-tuned on SST2 and RTE tasks using ZO and FO optimization methods with (✓) and without (✗) text alignment. The evident performance degradation is highlighted in bold.

Method	SST2			RTE		
	✓	✗	Difference	✓	✗	Difference
FO-SGD	91.6	91.5	0.1	70.9	61.4	9.5
ZO-SGD	89.4	79.2	10.2	68.7	60.4	8.3
ZO-Adam	89.8	79.2	10.6	69.2	58.7	10.5

ZO optimization methods. Additionally, we include ZO-SGD-MMT and ZO-SGD-Cons as they incorporate certain forms of ‘adaptive learning’ into the descent step updates. The former utilizes momentum based on historical gradient information, while the latter allows for the heuristics-based selection of the descent direction. Furthermore, ZO-Adam is one of the most complex ZO optimizers due to its utilization of moving averages and adaptive learning rates.

Task alignment in ZO optimization for LLM fine-tuning.

Scaling up ZO optimization for deep model training, as discussed in (Chen et al., 2024), is exceedingly challenging due to its high variance, which is dependent on the model size. Nevertheless, LLM pre-training offers a unique advantage by enabling the fine-tuner to start from a well-optimized pre-trained model state. This graceful model initialization makes ZO optimization potentially scalable to LLM fine-tuning tasks (Malladi et al., 2023). Even in this pretraining-finetuning paradigm, another crucial factor, which we call ‘**task alignment**’, still plays a key role in achieving satisfactory ZO fine-tuning performance. The ‘task alignment’ refers to aligning the fine-tuning task with the format of the pre-training task, given by the next token or sentence prediction. For example, Gao et al. (2020); Malladi et al. (2023) have transformed downstream text classification tasks into next token prediction tasks by introducing well-crafted input prompts. These prompts serve as bridges to align the fine-tuning tasks with the pre-training ones, facilitating ZO optimization when initiated from the pre-trained model.

As a warm-up experiment, **Tab. 1** empirically justifies the importance of task alignment when applying ZO optimization to LLM fine-tuning on the simple binary classification task by comparing scenarios *with* and *without* the use of pre-defined prompts to achieve task alignment. We fine-tune the entire Roberta-Large (Liu et al., 2019b) model on SST2 (Socher et al., 2013) and RTE (Wang et al., 2019) datasets with two selected ZO methods: ZO-SGD (*i.e.*, MeZO in (Malladi et al., 2023)) and ZO-Adam. We compare their performance with that of the FO method (FO-SGD). The task alignment is achieved with the template <CLS>SENTENCE. It was [terrible|great].<SEP> for SST dataset and another template <CLS>SENTENCE1? [Yes|No], SENTENCE2.<SEP> for RTE. As we can see, without

prompt-based text alignment, there is a substantial performance drop across ZO fine-tuning methods. Both ZO-SGD and ZO-Adam yield about 10% and 8% accuracy degradation on SST2 and RTE, respectively. In contrast, FO-SGD suffers less from the absence of task alignment. This suggests that the task alignment is particularly beneficial to ZO LLM fine-tuning. It is also worth noting that crafting effective prompts for task alignment can be non-trivial, as prompt design is context-dependent and can affect the fine-tuning performance. In this work, we follow (Gao et al., 2020) and (Malladi et al., 2023) to align the fine-tuning tasks to the pretrained ones.

4. Benchmarking ZO Optimization for LLM Fine-Tuning

In this section, we delve into the empirical performance of ZO optimization in LLM fine-tuning. Our benchmarking effort includes evaluating accuracy and efficiency, accounting for different downstream task complexities (ranging from simple classification to more complicated reasoning task), and considering various language model types.

4.1. Benchmark Setups

LLM fine-tuning tasks, schemes, and models. We begin by introducing the tasks and the fine-tuning schemes. We focus on *three tasks*, considering their complexity from low to high, which include (1) the simplest binary classification task, Stanford Sentiment Treebank v2 (SST2) (Socher et al., 2013), (2) the question-answering task, Choice Of Plausible Alternatives (COPA) (Roemmele et al., 2011), and (3) the commonsense reasoning task, WinoGrande (Sakaguchi et al., 2021). When evaluating memory efficiency, we also consider the task of multi-sentence reading comprehension (MultiRC) (Khashabi et al., 2018). For LLM fine-tuning on these tasks, we explore *four parameter-efficient fine-tuning (PEFT) schemes*: full-tuning (FT) that fine-tunes the entire pre-trained model, low-rank adaptation (LoRA) by imposing low-rank weight perturbations (Hu et al., 2021a), prefix-tuning (Prefix) by appending learnable parameters to token embedding (Li & Liang, 2021), and prompt-tuning (Prompt) (Liu et al., 2022) by introducing a series of learnable tokens attached to the input to adapt the fixed model to downstream tasks. We refer readers to Appx. A for details. Furthermore, we incorporate several representative language models, including Roberta-Large (Liu et al., 2019b), OPT (Zhang et al., 2022a), LLaMA2 (Touvron et al., 2023), Vicuna (Zheng et al., 2023), and Mistral (Jiang et al., 2023).

Setup and implementation of ZO optimization. To train the previously mentioned LLM fine-tuners, we utilize the ZO optimization methods introduced in Sec. 3. These include ZO-SGD (*i.e.* MeZO (Malladi et al., 2023)), ZO-SGD-Sign, ZO-SGD-MMT, ZO-SGD-Cons, and ZO-Adam. For

Table 2. Performance of LLM fine-tuning on SST2 over pretrained Roberta-Large and OPT/1.3B. Best performance among ZO methods (including Forward-Grad) is highlighted in **bold**.

SST2	Roberta-Large				OPT-1.3B			
	FT	LoRA	Prefix	Prompt	FT	LoRA	Prefix	Prompt
FO-SGD	91.4	91.2	89.6	90.3	91.1	93.6	93.1	92.8
Forward-Grad	90.1	89.7	89.5	87.3	90.3	90.3	90.0	82.4
ZO-SGD	89.4	90.8	90.0	87.6	90.8	90.1	91.4	84.4
ZO-SGD-MMT	89.6	90.9	90.1	88.6	85.2	91.3	91.2	86.9
ZO-SGD-Cons	89.6	91.6	90.1	88.5	88.3	90.5	81.8	84.7
ZO-SGD-Sign	52.5	90.2	53.6	86.1	87.2	91.5	89.5	72.9
ZO-Adam	89.8	89.5	90.2	88.8	84.4	92.3	91.4	75.7

comparison, we also present the performance of Forward-Grad, which relies on the forward mode auto-differentiation rather than BP. We also provide the performance of two FO optimizers: (FO-)SGD and (FO-)Adam. Before applying the aforementioned optimizers to the LLM fine-tuning tasks, we follow (Gao et al., 2020; Malladi et al., 2023) to align the fine-tuning task format with the token or sentence prediction-based pre-training task, as demonstrated in Tab. 1. We run ZO (or BP-free) optimizers and FO optimizers for 20000 and 625 iterations respectively, as outlined in (2). Note that ZO optimization takes a longer convergence time as shown in (Liu et al., 2020). When implementing (RGE), unless specified otherwise, we set the query budget per gradient estimation to $q = 1$. We determine the values of other hyperparameters, such as the smoothing parameter and learning rate, through a grid search for each method. Following (Malladi et al., 2023), if not specified otherwise, we adopt the mixed precision (MP) training for FO optimizers, where the model is loaded with the full precision (*i.e.*, 32 bits) but training is carried out in half precision with 16 bits (FP16). For ZO optimizers, half-precision training is adopted throughout the model loading and training. We also remark that neither MP nor FP16 can be applied to Forward-Grad. We refer readers for more details to Appx. C.

Evaluation metrics. We evaluate ZO LLM fine-tuning using two sets of metrics: accuracy and efficiency. Accuracy measures the fine-tuned model’s test-time performance in specific tasks, such as test accuracy in classification tasks. Efficiency includes various measurements like memory efficiency (in terms of peak memory usage and GPU cost), query efficiency (*i.e.*, the number of function queries required for ZO optimization), and run-time efficiency. These metrics collectively provide insights into the resources needed for ZO LLM fine-tuning, helping assess its feasibility and cost-effectiveness in practical scenarios.

4.2. Experiment Results

ZO fine-tuning on SST2: A pilot study. In Tab. 2, experiments are conducted to compare the performance of different BP-free and BP-based (FO-SGD) methods on one of the simplest LLM downstream task: the binary classification task with SST2 dataset. We investigate two model architec-

tures, the medium-sized Roberta-Large and the larger model OPT-1.3B. Several key results are summarized below.

First, ZO-Adam seems to be the most effective ZO method, achieving the best performance in 4 out of 8 fine-tuning settings. However, as will be shown later, this is achieved at the cost of additional memory consumption. This is not surprising considering that ZO-Adam has the highest algorithmic complexity, as explained in Sec. 3.

Second, Forward-Grad is a competitive method compared to the ZO methods, especially in the FT (full-tuning) setting. This indicates that Forward-Grad may be suitable for problems of a larger scale, and make it a compelling baseline of ZO LLM fine-tuning. Additionally, when the complexity of the fine-tuning scheme decreases (*e.g.*, Prompt), the advantage of Forward-Grad over function value-based ZO methods diminishes.

Third, The performance of ZO methods exhibits high variance, as evidenced by the fluctuating relative rankings across different experimental scenarios, although extensive hyperparameter search efforts have been made. For example, the effectiveness of ZO-Adam degrades dramatically in the (OPT-1.3B, Prompt) setting. In addition, the MeZO method (*i.e.*, ZO-SGD) used in (Malladi et al., 2023) does *not* always emerge as the top-performing ZO optimizer for LLM fine-tuning across various settings. This variance is not surprising and could be largely attributed to the high variance of RGE (Nesterov & Spokoiny, 2017; Duchi et al., 2015).

Fourth, ZO-SGD-Cons and ZO-SGD-MMT also demonstrate strong performance as ZO optimizers in LLM fine-tuning. However, ZO-SGD-Sign, the simplest ZO optimization method, tends to be the weakest approach, except in the simplest fine-tuning setting Prompt. The above observations motivate us to extend our explorations, investigating the effectiveness of ZO methods across a broader spectrum of models and more complex tasks.

ZO fine-tuning on downstream tasks COPA and WinoGrande under OPT-13B. Extended from the experiments on SST2, Fig. 1 presents the fine-tuning performance on COPA and WinoGrande dataset using a larger model, OPT-13B. We summarize our key observations when the problem scales up and becomes more complicated.

First, compared to the previous results, the performance gap among different ZO methods are much enlarged. In the meantime, the performance gap between FO and ZO methods are also widened. For example, in the experiments with WinoGrande, the FO methods (FO-SGD and FO-Adam) outperform all the other ZO methods by a large margin. This observation shows the scalability bottleneck intrinsic to ZO methods, when dealing with larger models and/or more complex tasks.

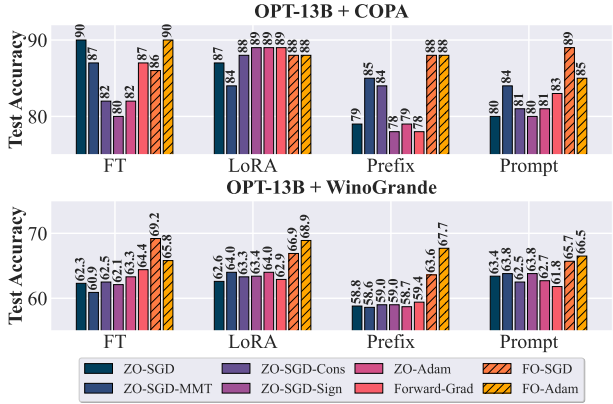


Figure 1. Results of OPT-13B on the tasks COPA and WinoGrande fine-tuned using ZO/FO optimizers in different PEFT settings.

Table 3. Performance of different LLMs finetuned with LoRA on COPA and WinoGrande using different ZO/FO methods. Table format is consistent with Tab. 2.

	OPT-13B	LLaMA2-7B	Vicuna-7B	Mistral-7B
COPA				
FO-SGD	88	85	84	90
FO-Adam	88	84	81	90
Forward-Grad	89	82	84	88
ZO-SGD	87	86	83	90
ZO-SGD-CONS	88	85	83	89
ZO-Adam	89	83	84	89
WinoGrande				
FO-SGD	66.9	66.9	66.5	76.4
FO-Adam	68.9	69.5	70.0	76.9
Forward-Grad	62.9	64.3	65.6	70.1
ZO-SGD	62.6	64.3	65.6	68.7
ZO-SGD-CONS	63.3	64.6	65.3	68.5
ZO-Adam	64.0	64.4	65.5	69.5

Second, certain ZO methods exhibit exceptional stability across varied conditions: Despite a general trend towards variability, specific ZO methods, *e.g.*, ZO-Adam and ZO-SGD-MMT, demonstrate stability in their performance. The reason for this could be that these algorithms integrate variance-reduced optimization techniques (such as momentum and adaptive learning rate) to ZO optimization and become more adaptable and resilient to the variances of ZO gradient estimation (Chen et al., 2019).

Third, the LoRA tuning method is consistently robust when paired with various ZO algorithms. This resilience across different ZO methods suggests that LoRA’s mechanism is inherently more adaptable to the variations in ZO optimization strategies, providing a stable and reliable tuning approach in diverse settings. We will peer into the performance of LoRA below.

In Tab. 3, we present how different ZO methods perform on

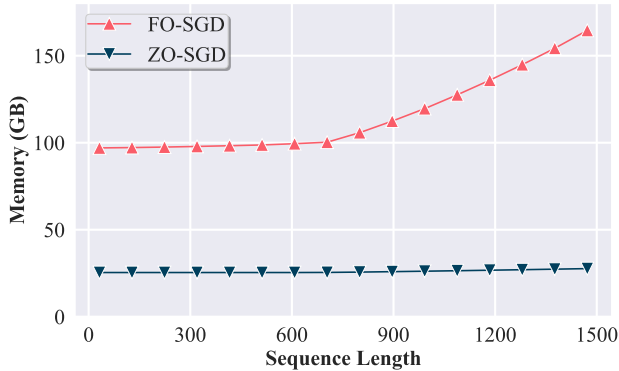


Figure 2. Memory comparison between FO-SGD and ZO-SGD full fine-tuning across various sequence lengths with a fixed effective batch size of 2. Memory evaluation was conducted using synthetic text generated from random sequences of the specified shapes. For shorter sequences (*i.e.*, < 700), the memory usage of FO-SGD remains relatively stable since the memory consumption for storing gradients during BP surpasses that needed for activations.

(LoRA, COPA) and (LoRA, WinoGrande) across a range of widely-used LLM families. For ease of computation, we focus on a subset of ZO optimization methods, including ZO-SGD, ZO-SGD-CONS, and ZO-Adam. As we can see, in some scenarios with the COPA dataset, some BP-free methods exhibit effectiveness comparable to, or even superior to, that of FO methods (FO-SGD and FO-Adam). For example, Forward-Grad and ZO-Adam outperform the best FO method on model OPT-13B and Vicuna-7B. Conversely, for the more difficult task WinoGrande, a performance gap of 5% ~ 6% between FO and ZO methods still exists across different models.

Efficiency analyses. In Tab. 4, we present a comparison of the efficiency performance of various ZO/FO optimizers when fine-tuning the full OPT-13B model on the MultiRC dataset with a batch size 4. We evaluate the efficiency in the following dimensions: memory cost (in GB), the consumption of GPU resources (number of GPUs), and runtime cost per optimization iteration (in seconds). All the experiments are carried out in the same environment. Several key observations can be made below.

First, almost all ZO methods (except ZO-Adam) demonstrate comparable levels of efficiency, requiring only a single GPU (A100) for LLM fine-tuning. This observation is expected as ZO methods entail relatively straightforward optimization steps, primarily based on function evaluations, as depicted in RGE. Among the examined ZO optimization methods, ZO-Adam incurs higher memory costs due to its algorithmic complexity. Second, in comparison to FO methods, ZO optimization reduces runtime costs per iteration, *e.g.*, by approximately 33.3% for ZO-SGD compared to FO-SGD. Third, Forward-Grad appears to be the point at which ZO optimization methods lose their memory efficiency advantage over FO methods. Additionally, we note that the

Table 4. The peak memory cost (in GB), the required GPU resources, and the runtime cost (in seconds) of each optimizer when fine-tuning the full OPT-13B model on MultiRC with an averaged 400 context length. The order of included optimizers is ranked based on the memory cost. The per-iteration runtime in seconds (s) is averaged over 100 iterations. Notably, Forward-Grad is marked by *, indicating its incompatibility with efficiency-enhancing techniques such as MP (mixed-precision training) and FP16 (half-precision training).

Optimizer	Memory ↓	Consumed GPUs ↓	Runtime Cost
ZO-SGD	29 GB	1×A100	1.8s
ZO-SGD-Cons	29 GB	1×A100	4.2s
ZO-SGD-Sign	29 GB	1×A100	1.8s
ZO-SGD-MMT	53 GB	1×A100	1.8s
ZO-Adam	80 GB	2×A100	1.9s
Forward-Grad*	138 GB	2×A100	19.8s
FO-SGD	161 GB	3×A100	2.7s
FO-Adam	257 GB	4×A100	2.8s

substantial runtime cost of Forward-Grad compared to FO optimizers (FO-SGD and FO-Adam) is possibly attributed to its incompatibility with MP and FP16.

Furthermore, we examine the memory cost of LLM fine-tuning vs. the input sequence length. In Fig. 2, we compare the memory efficiency between ZO-SGD and FO-SGD across various sequence lengths (*i.e.* the token number per sample). We employed synthetic texts generated from random sequences with specified shapes. In all experiments, an effective batch size of 2 was maintained. The memory consumption of ZO-SGD maintains a consistent level, whereas FO-SGD begins to demand significantly more memory as the sequence length extends. This trend is amplified particularly for longer sequences (*e.g.*, exceeding 700 as depicted in Fig. 2), where the memory allocated for activations overwhelms that required for gradient storage. We provide a theoretical analysis of this phenomenon in Appx C.

Ablation study on query budget. Recall from (1) that Forward-Grad provides us with an unbiased gradient estimate with respect to the FO gradient, in contrast to the function value-based biased ZO gradient estimate. However, in the above experiments, we have not observed a significant advantage brought by Forward-Grad. We hypothesize that this is due to the smallest query budget $q = 1$ we used, which, despite its query efficiency, may not fully showcase the unbiased benefit.

Inspired by the above, Fig. 3 explores the impact of varying query budget (q) on the performance of Forward-Grad and ZO-SGD (*i.e.*, MeZO). As we can see, both the accuracies of Forward-Grad and ZO-SGD are improved with an increased query budget. However, the performance rise for Forward-Grad is much more evident. For example, when the query number is larger than 500, Forward-Grad outperforms ZO-SGD by a large margin 1% ~ 2% and approaches FO-SGD. These observations underscore that the inherent advantages

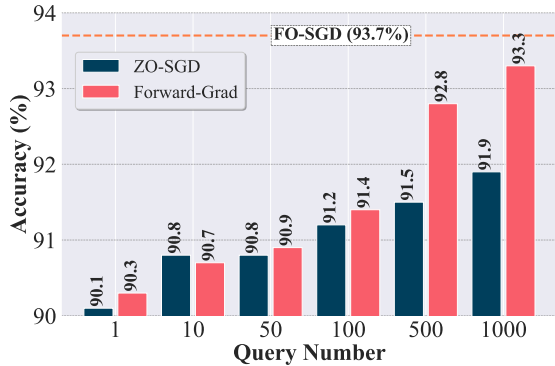


Figure 3. LoRA-based fine-tuning accuracy of OPT-1.3B on SST2 using ZO-SGD and Forward-Grad over different budgets.

of Forward-Grad become apparent only when a sufficient number of queries are used. The downside of using a higher query budget is the increase in computation cost, which scales linearly with q .

5. Extended Study to Improve ZO Fine-Tuning

Beyond the benchmarking effort in Sec. 4, we will explore algorithmic advancements to further improve the effectiveness of ZO LLM fine-tuning. We will leverage the following techniques: (1) *Block-wise ZO fine-tuning*; (2) *Hybrid ZO and FO fine-tuning*; and (3) *sparsity-induced ZO gradient estimation*. These designs aim to reduce the large variances in gradient estimation when using ZO algorithms.

Block-wise ZO optimization enhances fine-tuning performance.

It has been shown in (Liu et al., 2018) that using a coordinate-wise deterministic gradient estimator can reduce ZO optimization variance, although this scheme is difficult to scale. In a similar vein, we ask if RGE when estimating a FO gradient *block-wise* can also improve the performance of ZO optimization. The key idea is to split the LLM into different blocks and then apply the ZO gradient estimator to each block of parameters. For example, OPT-1.3B entails $p = 26$ parameter blocks, necessitating p forward passes for ZO gradient estimation per fine-tuning step. Our rationale is that by conducting gradient estimation block-wise, the resulting gradient estimate’s variance will be reduced, thereby potentially improving the fine-tuning performance.

In Tab. 5, we compare the performance of the ZO fine-tuning baseline MeZO (Malladi et al., 2023) (corresponding to ZO-SGD with a query budget of $q = 1$ in Sec. 4) with its block-wise RGE-based variant, which we term ZO-SGD-Block. For a fair comparison with ZO-SGD-Block in terms of query complexity, we also present the performance of another variant of ZO-SGD that uses the full model-wise RGE but takes the same query number q as ZO-SGD-Block per iteration. Notably, ZO-SGD-Block outperforms ZO-SGD in different query budget settings across different fine-

Table 5. Performance comparison of OPT-1.3B on the SST2 & WinoGrande tasks between ZO-SGD and ZO-SGD-Block. The # of parameter blocks in ZO-SGD-Block is set to $p = 26$. Thus, ZO-SGD w/ the query budget $q = 26$ has the same forward pass count as ZO-SGD-Block. MeZO corresponds to ZO-SGD w/ $q = 1$. Best performance for each task is highlighted in bold.

Optimizer	Forward Pass #	SST2	WinoGrande
MeZO	1	90.83	55.5
ZO-SGD ($q = 26$)	26	91.28	55.7
ZO-SGD-Block	26	93.69	57.2

tuning tasks, showing the benefit of *block-wise ZO tuning*.

Trade-off between performance and memory efficiency via hybrid ZO-FO training.

The primary source of memory cost in LLM fine-tuning arises from the BP process, which involves passing gradients from the deep layers to the shallow layers of the model. Hence, to enhance memory efficiency, a potential approach is to confine BP within the deep layers without propagating it to the shallow layers. Moreover, ZO optimization can be employed for the shallow layers without the need for BP. The above approach of combining FO optimization for deep layers and ZO optimization for shallow layers results in a *hybrid ZO-FO fine-tuning scheme* for LLMs.

Table 6. The trade-off between memory cost (in GB) v.s. fine-tuning accuracy (%) using the hybrid ZO-FO training on the OPT-1.3B model over the SST2 dataset. The memory or accuracy gap vs. that of the pure ZO-SGD method is noted by Δ .

ZO Layer #	Memory (GB)		Accuracy (%)	
	Memory	Δ Memory	Accuracy	Δ Accuracy
0 (FO-SGD)	24.29	11.07	91.22	1.98
4	23.33	10.11	91.12	1.88
8	22.01	8.79	90.79	1.55
12	20.43	7.21	89.48	0.24
16	18.98	5.76	89.42	0.18
20	15.43	2.21	89.27	0.03
24 (ZO-SGD)	13.22	0.00	89.24	0.00

Tab. 6 presents the performance of using the hybrid ZO-FO fine-tuning scheme on (OPT-1.3B, SST2). We examine different variants of this hybrid scheme by deciding ‘where’ to split between ZO optimization (for shallow layers) and FO optimization (for deep layers). Suppose that the model consists of n layers, and we designate the first $k \in [1, n]$ layers for ZO optimization, while the remaining $(n - k)$ layers are allocated for FO optimization. The pure ZO optimization approach corresponds to $p = n$. The results presented in Tab. 6 demonstrate that employing ZO optimization on only the first third of the model layers (*i.e.*, $k \leq 8$) can yield performance comparable to that achieved by fully utilizing FO optimization while also reducing memory usage by approximately 10%. Furthermore, when half of the layers employ ZO optimization (*i.e.*, $k \geq 12$), the performance achieved is similar to that of full ZO fine-tuning.

Table 7. Performance of fine-tuning OPT-1.3B on COPA & SST2 datasets using ZO-SGD at different sparsity ratios. A sparsity of 0% represents the baseline, the vanilla ZO-SGD, *i.e.*, MeZO (Malladi et al., 2023). Performance that surpasses the baseline (w/ 0% sparsity) is highlighted in **bold**.

		COPA									
Sparsity (%)		0	10	20	30	40	50	60	70	80	90
Accuracy (%)		73.00	75.00	75.00	70.00	70.00	70.00	70.00	7.000	70.00	71.00
		SST2									
Sparsity (%)		0	10	20	30	40	50	60	70	80	90
Accuracy (%)		90.83	91.51	92.20	92.32	91.74	92.43	92.43	92.20	91.51	92.66

Gradient pruning benefits performance. We next explore gradient pruning, a technique known for accelerating model training without compromising convergence (McDanel et al., 2022). Our key idea is to induce sparse parameter perturbations for reducing gradient estimation variance in RGE. We begin by leveraging magnitude-based pruning (Frankle & Carbin, 2018; Chen et al., 2020) to obtain the layer-wise sparsity ratios. We then generate random pruning masks (following these layer-wise sparsity ratios) and apply them to the weight perturbations in RGE per ZO fine-tuning step. **Tab. 7** shows the performance of the sparsity-induced ZO gradient estimation in LLM fine-tuning as a function of the overall sparsity ratio. It becomes evident that choosing a moderate sparsity ratio (*e.g.*, 20%) can lead to improved performance over the vanilla ZO optimizer, ZO-SGD.

6. Conclusion

This work explores the application of zeroth-order (ZO) optimization in fine-tuning large language models (LLMs). ZO optimization approximates gradients using loss differences, eliminating the need for back-propagation and activation storage. While MeZO (Malladi et al., 2023) has made strides in adapting ZO optimization for LLMs, understanding the full ZO landscape remains an open question. To achieve this, we broaden the scope by considering various ZO optimization methods, task types, and evaluation metrics. We conduct the first benchmark study of different ZO optimization techniques, shedding light on their accuracy and efficiency. We also uncover overlooked ZO optimization principles, such as task alignment and the role of forward gradient. Leveraging these insights, we propose techniques like block-wise descent, hybrid ZO and FO training, and gradient sparsity to enhance ZO optimization-based LLM fine-tuning. The proposed enhancements to ZO optimization enable us to further improve fine-tuning accuracy while maintaining memory efficiency.

7. Impact Statements

This paper aims to advance the optimization foundations of the memory-efficient fine-tuning of large language models (LLMs). Its potential impacts are contingent on how these fine-tuned LLMs are utilized. On the positive side, achiev-

ing memory efficiency during LLM fine-tuning could lead to significant reductions in energy consumption, contributing to the development of green AI and achieving improved performance in resource-constrained environments. However, there is a potential negative aspect in terms of misuse, as the fine-tuned models could be employed for generating misinformation, phishing attacks, or releasing copyrighted and private information. However, given the technical focus of this work, there are no specific societal consequences directly stemming from it that need to be highlighted here.

Bibliography

- Amari, S.-i. Backpropagation and stochastic gradient descent method. *Neurocomputing*, 5(4-5):185–196, 1993.
- Balasubramanian, K. and Ghadimi, S. Zeroth-order (non)-convex stochastic optimization via conditional gradient and gradient updates. *Advances in Neural Information Processing Systems*, 31, 2018.
- Baydin, A. G., Pearlmutter, B. A., Syme, D., Wood, F., and Torr, P. Gradients without backpropagation. *arXiv preprint arXiv:2202.08587*, 2022.
- Belouze, G. Optimization without backpropagation. *arXiv preprint arXiv:2209.06302*, 2022.
- Boopathy, A. and Fiete, I. How to train your wide neural network without backprop: An input-weight alignment perspective. In *International Conference on Machine Learning*, pp. 2178–2205. PMLR, 2022.
- Cai, H., Lou, Y., McKenzie, D., and Yin, W. A zeroth-order block coordinate descent algorithm for huge-scale black-box optimization. *arXiv preprint arXiv:2102.10707*, 2021.
- Cai, H., Mckenzie, D., Yin, W., and Zhang, Z. Zeroth-order regularized optimization (zoro): Approximately sparse gradients and adaptive sampling. *SIAM Journal on Optimization*, 32(2):687–714, 2022.
- Chai, Y., Wang, S., Sun, Y., Tian, H., Wu, H., and Wang, H. Clip-tuning: Towards derivative-free prompt learning with a mixture of rewards, 2022.
- Chen, A., Zhang, Y., Jia, J., Diffenderfer, J., Liu, J., Parasyris, K., Zhang, Y., Zhang, Z., Kailkhura, B., and Liu, S. Deepzero: Scaling up zeroth-order optimization for deep model training. *ICLR*, 2024.
- Chen, P.-Y., Zhang, H., Sharma, Y., Yi, J., and Hsieh, C.-J. Zoo: Zeroth order optimization based black-box attacks to deep neural networks without training substitute models. In *Proceedings of the 10th ACM workshop on artificial intelligence and security*, pp. 15–26, 2017.

- Chen, S., Ge, C., Tong, Z., Wang, J., Song, Y., Wang, J., and Luo, P. Adaptformer: Adapting vision transformers for scalable visual recognition. *Advances in Neural Information Processing Systems*, 35:16664–16678, 2022.
- Chen, T., Frankle, J., Chang, S., Liu, S., Zhang, Y., Wang, Z., and Carbin, M. The lottery ticket hypothesis for pre-trained bert networks. *Advances in neural information processing systems*, 33:15834–15846, 2020.
- Chen, X., Liu, S., Xu, K., Li, X., Lin, X., Hong, M., and Cox, D. Zo-adamm: Zeroth-order adaptive momentum method for black-box optimization. *NeurIPS*, 2019.
- Cheng, M., Singh, S., Chen, P. H., Chen, P.-Y., Liu, S., and Hsieh, C.-J. Sign-opt: A query-efficient hard-label adversarial attack. In *International Conference on Learning Representations*, 2020. URL <https://openreview.net/forum?id=Sk1TQCnTvS>.
- Cheng, S., Wu, G., and Zhu, J. On the convergence of prior-guided zeroth-order optimization algorithms. *Advances in Neural Information Processing Systems*, 34:14620–14631, 2021.
- Deng, M., Wang, J., Hsieh, C.-P., Wang, Y., Guo, H., Shu, T., Song, M., Xing, E. P., and Hu, Z. Rlprompt: Optimizing discrete text prompts with reinforcement learning, 2022.
- Dhurandhar, A., Pedapati, T., Balakrishnan, A., Chen, P.-Y., Shanmugam, K., and Puri, R. Model agnostic contrastive explanations for structured data. *arXiv preprint arXiv:1906.00117*, 2019.
- Duchi, J. C., Jordan, M. I., Wainwright, M. J., and Wibisono, A. Optimal rates for zero-order convex optimization: The power of two function evaluations. *IEEE Transactions on Information Theory*, 61(5):2788–2806, 2015.
- Flaxman, A. D., Kalai, A. T., and McMahan, H. B. Online convex optimization in the bandit setting: gradient descent without a gradient. *arXiv preprint cs/0408007*, 2004.
- Flaxman, A. D., Kalai, A. T., and McMahan, H. B. Online convex optimization in the bandit setting: Gradient descent without a gradient. In *Proceedings of the sixteenth annual ACM-SIAM symposium on Discrete algorithms*, pp. 385–394, 2005.
- Frankle, J. and Carbin, M. The lottery ticket hypothesis: Finding sparse, trainable neural networks. *arXiv preprint arXiv:1803.03635*, 2018.
- Gao, T., Fisch, A., and Chen, D. Making pre-trained language models better few-shot learners. *arXiv preprint arXiv:2012.15723*, 2020.
- Ghadimi, S. and Lan, G. Stochastic first-and zeroth-order methods for nonconvex stochastic programming. *SIAM Journal on Optimization*, 23(4):2341–2368, 2013.
- Gu, B., Liu, G., Zhang, Y., Geng, X., and Huang, H. Optimizing large-scale hyperparameters via automated learning algorithm. *arXiv preprint arXiv:2102.09026*, 2021a.
- Gu, J., Feng, C., Zhao, Z., Ying, Z., Chen, R. T., and Pan, D. Z. Efficient on-chip learning for optical neural networks through power-aware sparse zeroth-order optimization. In *Proceedings of the AAAI Conference on Artificial Intelligence*, volume 35, pp. 7583–7591, 2021b.
- Han, S., Mao, H., and Dally, W. J. Deep compression: Compressing deep neural networks with pruning, trained quantization and huffman coding. *arXiv preprint arXiv:1510.00149*, 2015.
- Hinton, G. The forward-forward algorithm: Some preliminary investigations. *arXiv preprint arXiv:2212.13345*, 2022.
- Hoffman, S. C., Chenthamarakshan, V., Wadhawan, K., Chen, P.-Y., and Das, P. Optimizing molecules using efficient queries from property evaluations. *Nature Machine Intelligence*, 4(1):21–31, 2022.
- Hogan, T. A. and Kailkhura, B. Universal decision-based black-box perturbations: Breaking security-through-obscure defenses. *arXiv preprint arXiv:1811.03733*, 2018.
- Houlsby, N., Giurgiu, A., Jastrzebski, S., Morrone, B., De Laroussilhe, Q., Gesmundo, A., Attariyan, M., and Gelly, S. Parameter-efficient transfer learning for nlp. In *International Conference on Machine Learning*, pp. 2790–2799. PMLR, 2019.
- Hu, E. J., Shen, Y., Wallis, P., Allen-Zhu, Z., Li, Y., Wang, S., Wang, L., and Chen, W. Lora: Low-rank adaptation of large language models, 2021a.
- Hu, S., Ding, N., Wang, H., Liu, Z., Wang, J., Li, J., Wu, W., and Sun, M. Knowledgeable prompt-tuning: Incorporating knowledge into prompt verbalizer for text classification. *arXiv preprint arXiv:2108.02035*, 2021b.
- Huang, F., Gao, S., Pei, J., and Huang, H. Accelerated zeroth-order and first-order momentum methods from mini to minimax optimization. *The Journal of Machine Learning Research*, 23(1):1616–1685, 2022.
- Ilyas, A., Engstrom, L., Athalye, A., and Lin, J. Black-box adversarial attacks with limited queries and information. In *International conference on machine learning*, pp. 2137–2146. PMLR, 2018.

- Jaderberg, M., Czarnecki, W. M., Osindero, S., Vinyals, O., Graves, A., Silver, D., and Kavukcuoglu, K. Decoupled neural interfaces using synthetic gradients. In *International conference on machine learning*, pp. 1627–1635. PMLR, 2017.
- Jiang, A. Q., Sablayrolles, A., Mensch, A., Bamford, C., Chaplot, D. S., Casas, D. d. l., Bressand, F., Lengyel, G., Lample, G., Saulnier, L., et al. Mistral 7b. *arXiv preprint arXiv:2310.06825*, 2023.
- Karimi Mahabadi, R., Henderson, J., and Ruder, S. Compacter: Efficient low-rank hypercomplex adapter layers. *Advances in Neural Information Processing Systems*, 34: 1022–1035, 2021.
- Khashabi, D., Chaturvedi, S., Roth, M., Upadhyay, S., and Roth, D. Looking beyond the surface: a challenge set for reading comprehension over multiple sentences. In *Proceedings of North American Chapter of the Association for Computational Linguistics (NAACL)*, 2018.
- Kim, B., Cai, H., McKenzie, D., and Yin, W. Curvature-aware derivative-free optimization. *arXiv preprint arXiv:2109.13391*, 2021.
- Kim, T., Kim, H., Yu, G.-I., and Chun, B.-G. BPipe: Memory-balanced pipeline parallelism for training large language models. In Krause, A., Brunskill, E., Cho, K., Engelhardt, B., Sabato, S., and Scarlett, J. (eds.), *Proceedings of the 40th International Conference on Machine Learning*, volume 202 of *Proceedings of Machine Learning Research*, pp. 16639–16653. PMLR, 23–29 Jul 2023.
- Kingma, D. P. and Ba, J. Adam: A method for stochastic optimization. *arXiv preprint arXiv:1412.6980*, 2014.
- Lester, B., Al-Rfou, R., and Constant, N. The power of scale for parameter-efficient prompt tuning, 2021.
- Li, X. L. and Liang, P. Prefix-tuning: Optimizing continuous prompts for generation, 2021.
- Lin, Z., Madotto, A., and Fung, P. Exploring versatile generative language model via parameter-efficient transfer learning, 2020.
- Liu, S., Kailkhura, B., Chen, P.-Y., Ting, P., Chang, S., and Amini, L. Zeroth-order stochastic variance reduction for nonconvex optimization. In *Advances in Neural Information Processing Systems*, volume 31, 2018.
- Liu, S., Chen, P.-Y., Chen, X., and Hong, M. signSGD via zeroth-order oracle. In *International Conference on Learning Representations*, 2019a.
- Liu, S., Chen, P.-Y., Kailkhura, B., Zhang, G., Hero III, A. O., and Varshney, P. K. A primer on zeroth-order optimization in signal processing and machine learning: Principals, recent advances, and applications. In *IEEE Signal Processing Magazine*, volume 37, pp. 43–54. IEEE, 2020.
- Liu, X., Ji, K., Fu, Y., Tam, W. L., Du, Z., Yang, Z., and Tang, J. P-tuning v2: Prompt tuning can be comparable to fine-tuning universally across scales and tasks. *arXiv preprint arXiv:2110.07602*, 2021.
- Liu, X., Ji, K., Fu, Y., Tam, W., Du, Z., Yang, Z., and Tang, J. P-tuning: Prompt tuning can be comparable to fine-tuning across scales and tasks. In *Proceedings of the 60th Annual Meeting of the Association for Computational Linguistics (Volume 2: Short Papers)*, pp. 61–68, 2022.
- Liu, Y., Ott, M., Goyal, N., Du, J., Joshi, M., Chen, D., Levy, O., Lewis, M., Zettlemoyer, L., and Stoyanov, V. Roberta: A robustly optimized bert pretraining approach. *arXiv preprint arXiv:1907.11692*, 2019b.
- Luo, G., Huang, M., Zhou, Y., Sun, X., Jiang, G., Wang, Z., and Ji, R. Towards efficient visual adaption via structural re-parameterization. *arXiv preprint arXiv:2302.08106*, 2023.
- Malladi, S., Gao, T., Nichani, E., Damian, A., Lee, J. D., Chen, D., and Arora, S. Fine-tuning language models with just forward passes. *arXiv preprint arXiv:2305.17333*, 2023.
- McDanel, B., Dinh, H., and Magallanes, J. Accelerating dnn training with structured data gradient pruning. In *2022 26th International Conference on Pattern Recognition (ICPR)*, pp. 2293–2299. IEEE, 2022.
- Meier, F., Mujika, A., Gauy, M. M., and Steger, A. Improving gradient estimation in evolutionary strategies with past descent directions. *arXiv preprint arXiv:1910.05268*, 2019.
- Nesterov, Y. and Spokoiny, V. Random gradient-free minimization of convex functions. *Foundations of Computational Mathematics*, 17:527–566, 2017.
- Nøkland, A. and Eidnes, L. H. Training neural networks with local error signals. In *International conference on machine learning*, pp. 4839–4850. PMLR, 2019.
- Ohta, M., Berger, N., Sokolov, A., and Riezler, S. Sparse perturbations for improved convergence in stochastic zeroth-order optimization. In *Machine Learning, Optimization, and Data Science: 6th International Conference, LOD 2020, Siena, Italy, July 19–23, 2020, Revised Selected Papers, Part II 6*, pp. 39–64. Springer, 2020.

- Pfeiffer, J., Rücklé, A., Poth, C., Kamath, A., Vulić, I., Ruder, S., Cho, K., and Gurevych, I. Adapterhub: A framework for adapting transformers. *arXiv preprint arXiv:2007.07779*, 2020.
- Prasad, A., Hase, P., Zhou, X., and Bansal, M. Grips: Gradient-free, edit-based instruction search for prompting large language models, 2023.
- Raffel, C., Shazeer, N., Roberts, A., Lee, K., Narang, S., Matena, M., Zhou, Y., Li, W., and Liu, P. J. Exploring the limits of transfer learning with a unified text-to-text transformer, 2023.
- Ren, J., Rajbhandari, S., Aminabadi, R. Y., Ruwase, O., Yang, S., Zhang, M., Li, D., and He, Y. Zero-offload: Democratizing billion-scale model training, 2021.
- Ren, M., Kornblith, S., Liao, R., and Hinton, G. Scaling forward gradient with local losses. *arXiv preprint arXiv:2210.03310*, 2022.
- Roemmele, M., Bejan, C. A., and Gordon, A. S. Choice of plausible alternatives: An evaluation of commonsense causal reasoning. In *2011 AAAI Spring Symposium Series*, 2011.
- Sakaguchi, K., Bras, R. L., Bhagavatula, C., and Choi, Y. Winogrande: An adversarial winograd schema challenge at scale. *Communications of the ACM*, 64(9):99–106, 2021.
- Sanh, V., Webson, A., Raffel, C., Bach, S. H., Sutawika, L., Alyafeai, Z., Chaffin, A., Stiegler, A., Scao, T. L., Raja, A., Dey, M., Bari, M. S., Xu, C., Thakker, U., Sharma, S. S., Szczechla, E., Kim, T., Chhablani, G., Nayak, N., Datta, D., Chang, J., Jiang, M. T.-J., Wang, H., Manica, M., Shen, S., Yong, Z. X., Pandey, H., Bawden, R., Wang, T., Neeraj, T., Rozen, J., Sharma, A., Santilli, A., Fevry, T., Fries, J. A., Teehan, R., Bers, T., Biderman, S., Gao, L., Wolf, T., and Rush, A. M. Multitask prompted training enables zero-shot task generalization, 2022.
- Shu, Y., Dai, Z., Sng, W., Verma, A., Jaillet, P., and Low, B. K. H. Zeroth-order optimization with trajectory-informed derivative estimation. In *The Eleventh International Conference on Learning Representations*, 2022.
- Silver, D., Goyal, A., Danihelka, I., Hessel, M., and van Hasselt, H. Learning by directional gradient descent. In *International Conference on Learning Representations*, 2021.
- Singhal, U., Cheung, B., Chandra, K., Ragan-Kelley, J., Tenenbaum, J. B., Poggio, T. A., and Yu, S. X. How to guess a gradient. *arXiv preprint arXiv:2312.04709*, 2023.
- Socher, R., Perelygin, A., Wu, J., Chuang, J., Manning, C. D., Ng, A. Y., and Potts, C. Recursive deep models for semantic compositionality over a sentiment treebank. In *Proceedings of the 2013 conference on empirical methods in natural language processing*, pp. 1631–1642, 2013.
- Sun, T., He, Z., Qian, H., Zhou, Y., Huang, X., and Qiu, X. Bbtv2: Towards a gradient-free future with large language models, 2022a.
- Sun, T., Shao, Y., Qian, H., Huang, X., and Qiu, X. Black-box tuning for language-model-as-a-service. In *International Conference on Machine Learning*, pp. 20841–20855. PMLR, 2022b.
- Tan, Z., Zhang, X., Wang, S., and Liu, Y. Msp: Multi-stage prompting for making pre-trained language models better translators. *arXiv preprint arXiv:2110.06609*, 2021.
- Touvron, H., Martin, L., Stone, K., Albert, P., Almahairi, A., Babaei, Y., Bashlykov, N., Batra, S., Bhargava, P., Bhosale, S., et al. Llama 2: Open foundation and fine-tuned chat models. *arXiv preprint arXiv:2307.09288*, 2023.
- Tsai, Y.-Y., Chen, P.-Y., and Ho, T.-Y. Transfer learning without knowing: Reprogramming black-box machine learning models with scarce data and limited resources. In *International Conference on Machine Learning*, pp. 9614–9624. PMLR, 2020.
- Tsaknakis, I., Kailkhura, B., Liu, S., Loveland, D., Diffenderfer, J., Hiszpanski, A. M., and Hong, M. Zeroth-order sciml: Non-intrusive integration of scientific software with deep learning. *arXiv preprint arXiv:2206.02785*, 2022.
- Tu, C.-C., Ting, P., Chen, P.-Y., Liu, S., Zhang, H., Yi, J., Hsieh, C.-J., and Cheng, S.-M. Autozoom: Autoencoder-based zeroth order optimization method for attacking black-box neural networks. In *Proceedings of the AAAI Conference on Artificial Intelligence*, pp. 742–749, 2019.
- Vemula, A., Sun, W., and Bagnell, J. Contrasting exploration in parameter and action space: A zeroth-order optimization perspective. In *The 22nd International Conference on Artificial Intelligence and Statistics*, pp. 2926–2935. PMLR, 2019.
- Verma, A., Bangar, S., Subramanyam, A., Lal, N., Shah, R. R., and Satoh, S. Certified zeroth-order black-box defense with robust unet denoiser. *arXiv preprint arXiv:2304.06430*, 2023.
- Vicol, P., Kolter, Z., and Swersky, K. Low-variance gradient estimation in unrolled computation graphs with es-single. *arXiv preprint arXiv:2304.11153*, 2023.

- Wang, A., Singh, A., Michael, J., Hill, F., Levy, O., and Bowman, S. R. GLUE: A multi-task benchmark and analysis platform for natural language understanding. In *International Conference on Learning Representations*, 2019.
- Wang, X., Guo, W., Su, J., Yang, X., and Yan, J. Zarts: On zero-order optimization for neural architecture search. *Advances in Neural Information Processing Systems*, 35: 12868–12880, 2022.
- Wang, Y., Du, S., Balakrishnan, S., and Singh, A. Stochastic zeroth-order optimization in high dimensions. *arXiv preprint arXiv:1710.10551*, 2017.
- Ye, H., Huang, Z., Fang, C., Li, C. J., and Zhang, T. Hessian-aware zeroth-order optimization for black-box adversarial attack. *arXiv preprint arXiv:1812.11377*, 2018.
- Zhang, S., Roller, S., Goyal, N., Artetxe, M., Chen, M., Chen, S., Dewan, C., Diab, M., Li, X., Lin, X. V., et al. Opt: Open pre-trained transformer language models. *arXiv preprint arXiv:2205.01068*, 2022a.
- Zhang, Y., Yao, Y., Jia, J., Yi, J., Hong, M., Chang, S., and Liu, S. How to robustify black-box ml models? a zeroth-order optimization perspective. *ICLR*, 2022b.
- Zhao, P., Liu, S., Chen, P.-Y., Hoang, N., Xu, K., Kailkhura, B., and Lin, X. On the design of black-box adversarial examples by leveraging gradient-free optimization and operator splitting method. In *Proceedings of the IEEE/CVF International Conference on Computer Vision*, pp. 121–130, 2019.
- Zheng, L., Chiang, W.-L., Sheng, Y., Zhuang, S., Wu, Z., Zhuang, Y., Lin, Z., Li, Z., Li, D., Xing, E., et al. Judging llm-as-a-judge with mt-bench and chatbot arena. *arXiv preprint arXiv:2306.05685*, 2023.
- Zhu, S., Voigt, T., Ko, J., and Rahimian, F. On-device training: A first overview on existing systems, 2023.

Appendix

A. Preliminaries of Parameter-Efficient Fine-Tuning (PEFT)

In our benchmark, we consider three PEFT methods, including {LoRA, prefix tuning, prompt tuning}.

1) *Low-Rank Adaptation (LoRA)*. LoRA modifies a pre-trained model by introducing trainable low-rank matrices, enabling fine-tuning with a limited parameter budget. Given a weight matrix $\mathbf{W} \in \mathbb{R}^{m \times n}$ in a transformer model, LoRA decomposes it as:

$$\mathbf{W}' = \mathbf{W} + \mathbf{B}\mathbf{A} \quad (\text{A1})$$

where \mathbf{W} is the original weight matrix, $\mathbf{B} \in \mathbb{R}^{m \times r}$ and $\mathbf{A} \in \mathbb{R}^{r \times n}$ are the low-rank matrices, and $r \ll \min(m, n)$ represents the rank. During fine-tuning, only \mathbf{B} and \mathbf{A} are updated, keeping \mathbf{W} frozen.

2) *Prompt Tuning*. Prompt tuning introduces a series of trainable tokens, or prompts, to guide the model's predictions. Let \mathbf{x} be the input sequence and $\mathbf{P} \in \mathbb{R}^{l \times d}$ the matrix representing the prompt embeddings, where l is the length of the prompt and d is the embedding dimension. The model input is then:

$$\hat{\mathbf{x}} = [\mathbf{P}; \mathbf{E}(\mathbf{x})] \quad (\text{A2})$$

where $\mathbf{E}(\mathbf{x})$ is the embedding of the original input \mathbf{x} , and $\hat{\mathbf{x}}$ represents the concatenated input of the prompt and the original input. During fine-tuning, only the prompt embeddings \mathbf{P} are learned, with the rest of the model parameters kept frozen.

3) *Prefix Tuning*. Prefix tuning extends the idea of prompt tuning to the attention mechanism of transformer models. Given an input sequence \mathbf{x} , the model processes it with additional context vectors \mathbf{C}_k and \mathbf{C}_v serving as keys and values in the attention mechanism:

$$\text{Attention}(\mathbf{Q}, \mathbf{K}, \mathbf{V}) = \text{softmax} \left(\frac{\mathbf{Q}(\mathbf{K} + \mathbf{C}_k)^T}{\sqrt{d_k}} \right) (\mathbf{V} + \mathbf{C}_v) \quad (\text{A3})$$

where \mathbf{Q} , \mathbf{K} and \mathbf{V} represent the query, key, and value matrices in the attention mechanism, $\mathbf{C}_k \in \mathbb{R}^{l \times d_k}$, $\mathbf{C}_v \in \mathbb{R}^{l \times d_v}$, and l is the length of the prefix. During training, only \mathbf{C}_k and \mathbf{C}_v are updated, and the original model parameters are frozen.

B. Zeroth-Order Optimization Algorithms

Zeroth-order optimization addresses the minimization or maximization of an objective function $f : \mathbb{R}^n \rightarrow \mathbb{R}$ without the use of derivatives:

$$\min_{\mathbf{x} \in \mathbb{R}^n} f(\mathbf{x})$$

These methods are pivotal when the function is non-differentiable, gradient computation is expensive, or the

function evaluations are noisy. Random gradient estimation (RGE) provides a surrogate for gradients in zeroth-order optimization by sampling function evaluations. The gradient $\nabla f(\mathbf{x})$ at a point \mathbf{x} can be approximated as:

$$\hat{\nabla} f(\mathbf{x}) := \frac{f(\mathbf{x} + \mu \mathbf{u}) - f(\mathbf{x} - \mu \mathbf{u})}{2\mu} \mathbf{u}$$

where \mathbf{u} is a standard Gaussian vector, and μ is a small scalar. This estimation facilitates the use of gradient-based methods solely based on function evaluations. Utilizing this gradient estimator, we summarize the existing zeroth-order algorithms below.

▷ *ZO-SGD* (Ghadimi & Lan, 2013). The method directly update the parameters by the estimated gradient:

$$\mathbf{x}_{t+1} = \mathbf{x}_t - \eta_t \hat{\nabla} f(\mathbf{x}_t),$$

where $\eta_t > 0$ is the learning rate.

▷ *ZO-SGD-Sign* (Liu et al., 2019a; Cheng et al., 2020). The intuition of ZO-SGD-Sign is to make the gradient estimation more robust to noise since the sign operation could mitigate the negative effect of (coordinate-wise) gradient noise of large variance. Yet, the downside of ZO-SGD-Sign is the lack of estimation precision. It is given by

$$\mathbf{x}_{t+1} = \mathbf{x}_t - \eta_t \text{sign} \left(\frac{f(\mathbf{x} + \mu \mathbf{u}) - f(\mathbf{x} - \mu \mathbf{u})}{2\mu} \mathbf{u} \right)$$

where \mathbf{u} is a standard Gaussian vector.

▷ *ZO-SGD-MMT* (Huang et al., 2022). The stochastic gradient estimated from a batch may suffer from a large variance. Momentum uses a moving average to estimate the global gradient and update the parameters by

$$\mathbf{x}_{t+1} = \mathbf{x}_t - \eta_t \mathbf{m}_t,$$

with the momentum defined as

$$\mathbf{m}_t = \beta_t \mathbf{m}_{t-1} + \hat{\nabla} f(\mathbf{x}_t).$$

ZO-SGD-MMT adopts the momentum factor β_t to control the average.

▷ *ZO-SGD-Cons* (Kim et al., 2021). This method is adapted from (Kim et al., 2021) to update the parameter conservatively: we pick up the point corresponding to the smallest loss value. The update is given by

$$\mathbf{x}_{t+1} = \arg \min_{\mathbf{y} \in \{\mathbf{x}_t, \mathbf{x}_t - \eta_t \hat{\nabla} f(\mathbf{x}_t), \mathbf{x}_t + \eta_t \hat{\nabla} f(\mathbf{x}_t)\}} f(\mathbf{y}).$$

▷ *ZO-Adam* (Chen et al., 2019). Similar to the ZO-SGD with momentum, ZO-Adam uses momentum to estimate the gradients. In addition, ZO-Adam adaptively penalizes the

learning rate to reduce the noise. The update of ZO-Adam is given by

$$\mathbf{x}_{t+1} = \mathbf{x}_t - \eta_t \frac{\sqrt{1 - \beta_2^t}}{1 - \beta_1^t} \mathbf{V}_t^{-1/2} \mathbf{m}_t,$$

where the momentum vector \mathbf{m} and the second-order momentum matrix \mathbf{V} are computed by

$$\begin{aligned} \mathbf{m}_t &= \beta_1 \mathbf{m}_{t-1} + (1 - \beta_1) \hat{\nabla} f(\mathbf{x}_t), \\ \mathbf{v}_t &= \beta_2 \mathbf{v}_{t-1} + (1 - \beta_2) [\hat{\nabla} f(\mathbf{x}_t)]^2, \\ \mathbf{V}_t &= \text{Diag}(\mathbf{v}_t). \end{aligned}$$

The hyperparameters β_1 and β_2 are used to control the moving average. Note ZO-Adam proposed in (Chen et al., 2019) differs from our implementation mainly by the RMSProp, *i.e.*, $\mathbf{v} = \max(\mathbf{v}_t, \mathbf{v}_{t-1})$. We remove RMSProp since it increases the memory cost and could void the advantage of ZO methods compared to FO-SGD.

▷ *Forward-Grad* (Baydin et al., 2022). Forward-Grad relies on the directional derivative along a random direction vector. Different from ZO optimization methods, it provides an unbiased stochastic gradient estimator of the FO gradient. The update of Forward-Grad is given by

$$\mathbf{x}_{t+1} = \mathbf{x}_t - \eta_t (\nabla f(\mathbf{x}_t)^\top \mathbf{u}) \mathbf{u},$$

where \mathbf{u} is the standard Gaussian random vector. While Forward-Grad utilizes the first-order gradient $\nabla f(\mathbf{x}_t)$, it employs the Jacobian-Vector Product during the forward pass of training to mitigate computation and memory requirements. As a result, the memory complexity remains relatively low compared to BP-based methods.

C. How to Implement Memory-Efficient ZO/FO Optimizers?

The memory efficiency of an optimizer heavily depends on its implementation details. This section will discuss these implementation details and provide a holistic memory profile of all the optimizers discussed above. We remark that the discussions in this section are based on the PyTorch framework.

In general, the memory efficiency of an optimizer is defined by the peak memories consumed during training in a specific setting, which primarily depends on the maximum number of variables stored at a certain time point. To dissect the memory consumption of different optimizers, we summarized a general model pipeline for parameter updating in Algorithm A1, which involves four main steps.

First, the program needs to load the model with the full parameters (\mathbf{x}) with either full or half-precision. This is an inevitable consumption for all optimizers. *Second*, a

Algorithm A1 A General Pipeline for A FO/ZO Optimizer

Input: Model with forward function f , parameters \mathbf{x} , previous optimizer state \mathbf{s}_{opt}

Memory Overview: \mathbf{s} : States of optimizer/model, τ : Temporary variables (*e.g.*, for copy/paste)

Step 0: Model Loading: Initialize the model with parameter \mathbf{x} ;

Step 1: Forward Pass: Compute loss $\ell(x)$, and save forward pass states \mathbf{s}_{fwd} ;

Step 2: Backward Pass: Calculate gradients *w.r.t.* \mathbf{x} , and generate backward states \mathbf{s}_{bwd} ;

Step 3: Optimization Step: Update \mathbf{x} and \mathbf{s}_{opt} using gradients and utilize temporal state \mathbf{s}'_{opt} that will be released immediately;

Output: Loss ℓ , updated parameters \mathbf{x} , and optimizer state \mathbf{s}_{opt} .

forward pass will yield a loss value and store any involved intermediate states of the model (\mathbf{s}_{fwd}). *Third*, the loss in a backward mode utilizes the stored state \mathbf{s}_{fwd} . Similarly, this BP process involves storing the backward states \mathbf{s}_{bwd} and temporarily storing τ_{bwd} . After the gradients and state \mathbf{s}_{bwd} are computed, the memory cost from \mathbf{s}_{fwd} will be immediately released. *Last*, with the computed gradient and states, the parameters and optimizer state will be updated, and the memory of \mathbf{s}_{bwd} will be released. Typically, \mathbf{s}_{bwd} will be the stored gradients. For generality, we assume \mathbf{s}_{fwd} also includes essential temporal variables that are only used in the step.

According to the memory life-cycle, the memory consumption will be summarized as two types: *constant memory* that exists through the training, and *dynamic allocation* that only exists in one iteration mainly for gradient computing. Though dynamic allocation only exists temporarily, it also contribute to the peak memory. Without losing generality, we summarize the primary components of the peak memory consumption as

$$\underbrace{|\mathbf{x}| + |\mathbf{s}_{\text{opt}}|}_{\text{constant}} + \underbrace{\max\{|\mathbf{s}_{\text{fwd}}|, |\mathbf{s}_{\text{bwd}}|, |\mathbf{s}'_{\text{opt}}|\}}_{\text{dynamic allocation}},$$

where $|\cdot|$ denotes the cardinality of a vector. Note that we concentrate on the primary factors in Big O notation, which, unless specified otherwise, was omitted for brevity.

C.1. Prevalent Efficiency-Enhancing Tricks Adopted in This Work

Prior to delving into the dissection of the memory consumption of different optimizers, we first introduce the prevalent efficiency-enhancing tricks widely adopted in the state-of-the-art FO/ZO-optimizers. These methods are by default adopted in this work if compatible to achieve the state-of-

the-art performance.

Half-precision training (FP16). Most modern LLMs, *e.g.* LLaMA2 (Touvron et al., 2023), operate at half-precision (*i.e.*, 16-bit) for inference, denoted as FP16. With FP16, only half of the model memory is required for ZO methods. By default, ZO methods are loaded at half-precision if the methods do not necessitate differentiation. However, as the current auto-differentiation module in PyTorch does not support FP16, methods like Forward-Grad must run at full precision. Similarly, for FO methods, half-precision is not compatible for the same reason.

Mixed-precision training (MP). Mixed precision is a common practice to speed up gradient computation by back-propagation. By default, MP is used in FO methods (FO-SGD and FO-Adam), where the model is loaded in full precision and the training is carried out in half-precision. Specifically, a half-precision replica of the model is used to conduct a forward pass yielding the intermediate results and gradients in half-precision. From the half-precision one, a full-precision gradient will be recovered for optimization. If the intermediate results consume more memory consumption than the model and gradients themselves, MP can also reduce memory complexity. We remark that MP is still operating on a full-precision model, which means MP and FP16 cannot be used together in PyTorch.

The ‘foreach’ implementation of Adam. The PyTorch implementation of Adam will use so-called foreach implementation to speed up the computation. At a high level, the foreach implementation will replicate and merge all the layers’ weight into one tensor during Adam updates. Operations on the unified tensor can be easily parallelized and therefore are faster. Though foreach can speed up computation, it demands extra memory to store all the weights.

C.2. Unpacking Memory Costs of Different Optimizers

In this section, we look into the optimizers studied in this work. For each algorithm, we will first analyze their theoretical memory consumption following the step 1 ~ 3 depicted in the framework in Algorithm A1. In the end, we provide a comparison between the theoretical and empirical results.

In most backward algorithms, activation \mathbf{a} will be cached for backward computation. We use $\bar{\mathbf{a}}$ and $\bar{\mathbf{x}}$ to denote the 16-bit version of \mathbf{a} and \mathbf{x} (half-precision), respectively. For all FO methods, the memory of the model parameters is of size $|\mathbf{x}|$. For all ZO methods with FP16, the memory of parameters is halved as $\frac{1}{2}|\mathbf{x}|$. Next, we will focus on the memory dynamics in Step 1-3.

FO-SGD (MP). In Step 1, the forward pass will first replicate the model in half-precision, *i.e.* $\bar{\mathbf{x}}$, leading to an extra memory consumption $\frac{1}{2}|\mathbf{x}|$. Then, the activation per layer will be cached as half-precision intermediate results,

$\bar{\mathbf{a}} = \oplus_{l=1}^L \bar{\mathbf{a}}_l$. In Step 2, the backward pass will compute the 16-bit gradient using activation per layer. The computation happens layer by layer. Therefore, the peak memory will be summed as $\sum_l \max\{\frac{1}{2}|\mathbf{a}_l|, |\mathbf{x}_l|\}$. For simplicity, we approximate the term as $\max\{\frac{1}{2}|\mathbf{a}|, |\mathbf{x}|\}$. In Step 3, there will be no optimization state. We can approximate the dynamic memory as

$$\begin{aligned} & \max\left\{\frac{1}{2}|\mathbf{a}| + \frac{1}{2}|\mathbf{x}|, \max\left\{\frac{1}{2}|\mathbf{a}|, |\mathbf{x}|\right\}\right\} \\ &= \max\left\{\frac{1}{2}|\mathbf{a}| + \frac{1}{2}|\mathbf{x}|, |\mathbf{x}|\right\}. \end{aligned}$$

The total memory consumption will be approximated as

$$\max\left\{\frac{1}{2}|\mathbf{a}| + \frac{3}{2}|\mathbf{x}|, 2|\mathbf{x}|\right\}.$$

FO-Adam (MP). In Step 1 and 2, FO-Adam completes the forward pass in the same way as FO-SGD and thus consumes memory similarly. In Step 3, the PyTorch Adam utilizes the ‘foreach’ implementation to speed up state computation. The Adam optimizer will first replicate the gradient in an extra memory of size $|\mathbf{x}|$. The replica will co-exist with the gradient in the memory temporarily, leading to a total memory $2|\mathbf{x}|$. Therefore, the peak memory will be the maximum of the dynamic memory in all of the three steps:

$$\begin{aligned} & \max\left\{\frac{1}{2}|\mathbf{a}| + \frac{1}{2}|\mathbf{x}|, \max\left\{\frac{1}{2}|\mathbf{a}|, |\mathbf{x}|\right\}, 2|\mathbf{x}|\right\} \\ &= \max\left\{\frac{1}{2}|\mathbf{a}| + \frac{1}{2}|\mathbf{x}|, 2|\mathbf{x}|\right\}. \end{aligned}$$

In addition to the dynamic memory, the optimization step adds two states in memory for first-order and second-order momentum vectors, *i.e.*, \mathbf{m}_t and \mathbf{v}_t . We can sum up the memory of all steps to estimate the total memory as

$$\max\left\{\frac{1}{2}|\mathbf{a}| + \frac{7}{2}|\mathbf{x}|, 5|\mathbf{x}|\right\}.$$

ZO-SGD (FP16). In Step 1-2, ZO-SGD estimates the gradient by two forward loss calculations based on the random direction vector \mathbf{u} . Yet, storing \mathbf{u} will be as costful as the whole model parameter. To reduce the consumption, the per-layer perturbation \mathbf{u}_l is computed on demand. For this purpose, we follow (Malladi et al., 2023) to use the random seed trick. Note the perturbation of all parameters is done sequentially and therefore we use random seed \mathcal{S} to reproduce the random direction vectors in the same order. Specifically, we initialize a random number generator by $\text{rng} = \text{RandomState}(\mathcal{S})$. Sequentially, we compute the random vector for a specific parameter \mathbf{x}_l by

$$\mathbf{u}_l \sim \mathcal{N}_{\text{mg}}(\mathbf{0}, \mathbf{I}),$$

where \mathcal{N}_{mg} represent the Gaussian distribution with the generator rng . In Step 3, we can also reproduce the random

vectors for computing the parameter gradient and immediately update \mathbf{x}_l . Without optimizer states, ZO-SGD consume a total memory as

$$\frac{1}{2}|\mathbf{x}| + \max_l |\mathbf{u}_l| = \frac{1}{2}|\mathbf{x}| + \max_l |\mathbf{x}_l|,$$

where the second term is the maximal dynamic memory with the random seed trick.

ZO-SGD-MMT (FP16). ZO-SGD with Momentum is similar to ZO-SGD, but it consumes extra memory for momentum storage. The momentum shares the same size as the model parameter. According to the memory of ZO-SGD, we can get the memory estimation as

$$|\mathbf{x}| + \max_l |\mathbf{x}_l|.$$

ZO-Adam (FP16). Similar to ZO-SGD-MMT, ZO-Adam has extra optimizer states, first-order and second-order momentum. They have the same memory consumption as the parameters. Therefore, the total estimated memory is

$$\frac{3}{2}|\mathbf{x}| + \max_l |\mathbf{x}_l|.$$

Forward-Grad. In Step 1 and 2, Forward-Grad estimates the gradient in one unified pass. Different from other ZO methods, Forward-Grad leverages the forward-mode auto-differentiation module¹ in PyTorch to estimate the directional derivative, *i.e.*, $\nabla f(\mathbf{x})^\top \mathbf{u}$. Therefore, we have to create and maintain the random vector \mathbf{u} for all parameters causing the memory in $|\mathbf{x}|$ size. In addition, Forward-Grad needs to forward the per-layer product of the Jacobian of activation *w.r.t.* the parameter and the random vector to the next layer. Therefore, there will be an additional memory cost per layer with the size of $|\mathbf{a}_l|$. In Step 3, Forward-Grad directly uses the gradient to update the parameters without extra memory costs. Thus, with the model memory, the total memory estimation can be summed as

$$2|\mathbf{x}| + \max_l |\mathbf{a}_l|.$$

C.3. Theoretical Memory Cost Comparison

In this section, we provide some analysis based on the theoretical results discussed above. In particular, we first summarize the theoretical memory efficiency of different optimizers in **Tab. A1**. Several key insights can be summarized. **First**, compared to FO optimizers (including Forward-Grad), the memory efficiency merits of ZO optimizers are mainly in two aspects. On the one hand, ZO can avoid saving the intermediate results (model states) \mathbf{a}_l . As discussed in **Fig. 2**, this reduction is considerable when the sequence length of the language model is large. On the other hand,

¹https://pytorch.org/tutorials/intermediate/forward_ad_usage.html

Table A1. Comparison of total memory complexity of different optimizers when fine-tuning the full model. $|\mathbf{x}|$ denotes the memory of parameters (or gradients in the same size) in full precision. $|\mathbf{a}|$ denotes the memory consumption of intermediate results saved for post-hoc backward during forward. $|\mathbf{x}_l|$ and $|\mathbf{a}_l|$ represents the parameter and intermediate memory of a specific layer l .

Optimizer	Memory
FO-SGD	$ \mathbf{x} + \max \left\{ \frac{1}{2} \mathbf{a} + \frac{1}{2} \mathbf{x} , \mathbf{x} \right\}$
FO-Adam	$3 \mathbf{x} + \max \left\{ \frac{1}{2} \mathbf{a} + \frac{1}{2} \mathbf{x} , 2 \mathbf{x} \right\}$
Forward-Grad	$ \mathbf{x} + \mathbf{x} + \max_l \mathbf{a}_l $
ZO-SGD	$\frac{1}{2} \mathbf{x} + \max_l \frac{1}{2} \mathbf{x}_l $
ZO-SGD-MMT	$ \mathbf{x} + \max_l \frac{1}{2} \mathbf{x}_l $
ZO-Adam	$\frac{3}{2} \mathbf{x} + \max_l \frac{1}{2} \mathbf{x}_l $

ZO method can estimate the gradient in a layer-wise sequential manner and thus avoid storing the gradients of the entire model. **Secondly**, in contrast to the half-precision (FP16) technique, the mixed precision (MP) training approach, which can be adopted by FO optimizers, solely diminishes the memory complexity associated with $|\mathbf{a}|$. It does not, however, reduce the memory consumption stemming from model loading or the storage of optimization states. In contrast, ZO can be equipped with FP16 with more flexibility, which helps achieves a memory reduction by 50%. **Third**, although Forward-Grad is also a BP-free method, its memory efficiency advantage over other FO optimizers is not remarkable. This is mainly due to its requirement for storing the intermediate results (*i.e.*, $|\mathbf{a}_l|$). In the meantime, Forward-Grad is not compatible with the modern efficiency enhancing tricks (such as FP16 or MP), which further reduces its memory efficiency. **Last**, although ZO-Adam is memory intensive compared to ZO-SGD, it can be greatly improved by using FP16, which shows a better efficiency than FO-SGD (MP).

Theoretical analysis on the memory consumption change with sequence length. We remark that the empirical results ($|\mathbf{a}|$) in **Tab. A1** are dependent on the input sequence length. In general, a larger sequence length will directly lead to a larger activation memory consumption. To investigate its impact, we explored how the scaling of input sequence length impacts memory usage by increasing activation memory in **Fig. 2**. **First**, when the sequence length is small (less than 700), the total memory overhead remains approximately the same when the sequence length increase. This is primarily due to that the theoretical memory consumption for FO-SGD is $|\mathbf{x}| + \max \left\{ \frac{1}{2}|\mathbf{a}| + \frac{1}{2}|\mathbf{x}|, |\mathbf{x}| \right\}$ (see **Tab. A1** for a reference) and the memory utilized by activations is less than that used for gradients. **Second**, as ZO-SGD does not need to store activations with a memory consumption of $\frac{1}{2}|\mathbf{x}| + \max_l \frac{1}{2}|\mathbf{x}_l|$, it exhibits a much better efficiency advantage over FO-SGD, when the sequence length increases (*e.g.*, 1504). Therefore, the memory efficiency gap shown in **Tab. 4** will be further enlarged if a larger input sequence length is used.